Nonlinear Phenomena in Systems of Magnetic Holes

Geir Helgesen,[1] Piotr Pieranski,[2] and Arne T. Skjeltorp[3]
[1]*Department of Physics, University of Oslo, N-316 Oslo 3, Norway*
[2]*Institute of Molecular Physics, Polish Academy of Sciences, Smoluchowskiego 17/19, 60-179 Poznan, Poland*
[3]*Institute of Energy Technology, N-2007 Kjeller, Norway*
(Received 5 September 1989)

Experimental studies are made of the response of bound pairs of magnetic holes (nonmagnetic microspheres in ferrofluid) subjected to a rotating magnetic field. For increasing driving frequency, the motion of the system goes through a transition from a state where the pair axis follows the magnetic field with a constant phase delay to a state where the phase delay increases in a series of kinks. The equation of motion for the rotating pair is found analytically and numerical solutions show good agreement with experiments.

PACS numbers: 75.10.−b, 75.50.Mm, 82.70.Dd

The dynamic and static properties of fine ferromagnetic particles in a viscous nonmagnetic medium are of wide interest in science and technology. Phenomena which occur in such systems are important in manufacturing of magnetic devices,[1] applications of ferrofluids,[2] and use of magnetic microspheres in medicine.[3] Numerous theoretical and numerical investigations have been made of the motion of single spherical and nonspherical particles in alternating magnetic fields,[4-6] but there are very few direct experimental observations on such systems.

The present paper reports novel experimental and numerical studies of the nonlinear response of bound pairs of magnetic holes[7,8] (microspheres in ferrofluid) confined between two parallel glass plates when subjected to rotating magnetic fields in the plane (Fig. 1). In contrast to ordinary magnetized particles with fixed moments, magnetic holes possess variable magnetic moments *collinear* with an external field at any strength. This combined with the possibility of direct microscopic observations of particle movements thus allows direct comparison of theory and experiments for a well defined model system to study nonlinear dynamics. The interplay between magnetic and viscous forces leads to various modes of motion (Fig. 2), which may be classified as (i) steady-state rotations; (ii) "jerky" (rotations with stops and backward motions); and (iii) localized oscillations depending on the frequency and amplitude of the rotating field, fluid viscosity, and magnetic susceptibility. As

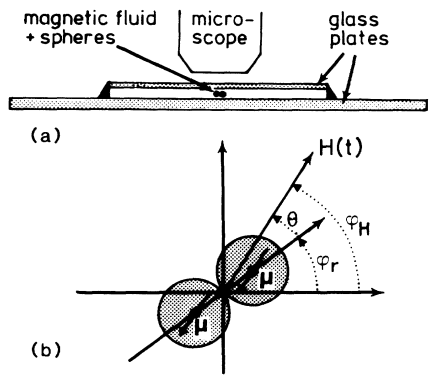

FIG. 1. (a) Sideview of the experimental setup. (b) Topview of the coordinate system for two magnetic holes rotating in the plane between the two glass plates in (a) and driven by the planar field $H(t)$ as discussed in the text.

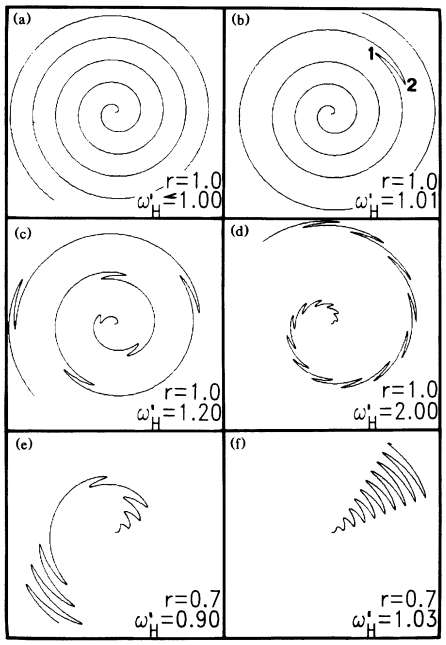

FIG. 2. Polar plot of the pair angle φ_r vs time (radially) for different values of the normalized angular frequency $\omega'_H = \omega_H/\omega_{c1}^{\xi}$ and for different anisotropy r of the counterclockwise rotating magnetic field as explained in the text: (a) just below the transition ω_{c1}^{ξ} (mode $M\zeta$); (b)–(d) at various angular frequencies above transition (mode $M\xi$); (e) below ω_{c2}^{ξ} in the anisotropic case (mode $M\xi$); and (f) above the transition ω_{c2}^{ξ} (mode $M\zeta$). The initial conditions for all simulations were $\theta(t=0) = 0$.

shown below, the transitions between these modes are well described by a single nonlinear equation.

The experimental setup is shown schematically in Fig. 1(a). The sample cell (20×20 mm^2) contained one pair of uniformly sized polystyrene spheres[9] (diameter 10–100 μm) dispersed in kerosene-based ferrofluid[10] and confined between two glass plates. The spacing between the plates was typically twice the diameter of the spheres. It was possible to create one pair by starting with a very dilute dispersion and moving two spheres into position by using a small hand-held magnet. In order to simplify the experimental conditions for the present studies, the spheres were prepared in such a way that once in contact they stayed together.[11] A set of four coils was used to produce a magnetic field $H(t)$ rotating within the x-y sample plane. The components of the field were $H_x\sin(\omega_H t)$ and $H_y\sin(\omega_H t+\pi/2)$ with angular frequency ω_H. Both circular polarized ($r=H_y/H_x=1$) and elliptical polarized fields ($r\neq1$) were used. The motion of the spheres was observed in a light microscope with video-camera attachment and recorder. The frequencies of the various modes were low (≤1 Hz) and could easily be measured manually using a stopwatch.

The coordinate system used in the derivation of the equation of motion is shown in Fig. 1(b). The apparent magnetic moment carried by each sphere is given by $M_c=-V\chi_{\rm eff}H$, where $V=\pi d^3/6$ is the volume of the sphere with diameter d and $\chi_{\rm eff}$ is the effective volume susceptibility of the ferrofluid. $\chi_{\rm eff}$ is related to the bulk susceptibility χ by $\chi_{\rm eff}=\chi/(1-4\pi\chi/3)$.[7] Since the apparent magnetic moments carried by both spheres are equal and always parallel, the interaction energy between them is given to first order by the dipolar term

$$U(\theta)=M_c^2(1-3\cos^2\theta)/d^3\,, \tag{1}$$

where $\theta=\phi_H-\phi_r$ is the angle (phase lag) between the pair axis and the direction of the field.[12] As mentioned above, the pair axis is bound and then d is assumed to be constant.

The magnetic torque, $T_H=-dU(\theta)/d\theta$, acting on the pair is given by

$$T_H=-\epsilon A(t)\sin(2\theta)\,, \tag{2}$$

with

$$\epsilon=\pi^2\chi_{\rm eff}^2H_x^2d^3/12\,,$$

$$A(t)=\cos^2(\omega_H t)+r^2\sin^2(\omega_H t)\,,$$

and

$$r=H_y/H_x\,.$$

Apart from the magnetic torque T_H, the pair is subjected to a viscous torque, T_η, acting opposite to the direction of the motion,

$$T_\eta=-K\eta\,d\varphi_r/dt\,, \tag{3}$$

where η is the viscosity of the ferrofluid and K is a geometrical factor related to the sphere diameter.[13]

For uniform rotation the two torques T_H and T_η are in equilibrium. Thus, the equation of motion for the rotating pair can be written as

$$d\varphi_r/dt=\omega_c A(t)\sin[2(\phi_H-\phi_r)]\,, \tag{4}$$

where $\omega_c=\epsilon/K\eta$ and $\varphi_H=\tan^{-1}[r\tan(\omega_H t)]$. In the reasoning given above, we have neglected the inertia term $I\,d^2\varphi_r/dt^2$. This can be done as the moment of inertia is small and the viscosity of the ferrofluid is high.

As discussed in the following all the experimental observations can be explained in terms of analytical and numerical solutions of the nonlinear Eq. (4). To facilitate a direct comparison between observations and numerical simulations, the latter will be presented in the form of polar $\varphi_r(t)$ plots. The starting condition for the numerical runs was always located on the steady-state trajectories referred to below as modes of motion. However, due to the strong damping, the initial transients were always relatively short (except when ω_H approached any of the critical frequencies we shall consider).

For the circular polarized field ($r=1$), direct observations show that there exist two distinctly different steady-state modes of motion. In the first mode (denoted by M_1^c), the bound pair is seen to rotate uniformly with frequency equal to that of the field. This occurs below a well defined frequency ω_{c1}^c of the rotating field. The numerical solution of Eq. (4) for this case is shown in Fig. 2(a). The simulations start with $H(t=0)$ coinciding with the pair axis. Asymptotically, a constant phase lag $\theta^0(\omega_H)$ develops and the motion of the pair becomes *phase locked* to the rotating field. The magnitude of the phase lag can easily be found by setting $d\varphi_r/dt=0$ in Eq. (4) yielding

$$\theta^0(\omega_H)=\tfrac{1}{2}\sin^{-1}(\omega_H/\omega_{c1}^c)\,. \tag{5}$$

The motion of the bound pair changes character as ω_H crosses a critical ω_{c1}^c value. This new mode is denoted by M_2^c. Here, the rotation of the pair is no longer uniform. What we observe instead is a periodic sequence of forward and backward rotations. For ω_H just above ω_{c1}^c, the forward rotations last much longer than the backward ones. As ω_H increases, they become more frequent and comparable in length. On average, the bound pair rotates in the same direction as the rotating field but the angular frequency $\bar{\omega}_r$ of this average motion goes to zero as $\omega_H\rightarrow\infty$. Measurements show that $\bar{\omega}_r\sim\omega_H^{-1}$ for $\omega_H\gg\omega_{c1}^c$. The critical frequency ω_{c1}^c, which separates the M_1^c mode from the M_2^c mode, is proportional to the square of the magnitude of the rotating field.

The numerical solutions of Eq. (4) for this case are shown in Figs. 2(b) and 2(c) where the forward-backward motion cycles are clearly seen. Simultaneous observation of both the magnetic-field direction and that of

the rotating pair reveal that the backward-motion intervals occur when the field makes the phase lag $\theta(t) \bmod(\pi)$ cross the $\pi/2$ value. At this point the magnetic torque changes sign, reversing the direction of the pair rotation. This lasts as long as $\theta(t) \bmod(\pi) \in (\pi/4, \pi)$. The cycle ends when the field and pair axis again coincide.

As may be seen in Fig. 2(d) for $\omega_H \gg \omega_{c1}^c$ the average motion of the pair axis approaches a well defined path. By integrating Eq. (4) (for $r=1$) from the end of one backward rotation to the end of the next, one finds that the angular frequency of the backward rotation is

$$\omega_b = 2\pi \Big/ \int_0^{\pi} \frac{d\theta}{\omega_H + \omega_{c1}^c \sin 2\theta} = 2\omega_H [1 - (\omega_{c1}^c/\omega_H)^2]^{1/2} \quad (6)$$

and thus $\omega_b \simeq 2\omega_H$ for $\omega_H \gg \omega_{c1}^c$. This is in close agreement with experimental observations. Equation (6) also shows that as ω_H approaches ω_{c1}^c from above, ω_b drops to zero. For this M_2^c mode the phase lag increases continuously via a sequence of kinks. For an elliptical rotating field ($H_x \neq H_y$), both M_1^c and M_2^c modes change their patterns. Rotations of the bound pair become modulated for low frequencies ω_H. In spite of the modulation, the average frequency of rotation is still equal to ω_H. Let us denote this mode by M_1^e. (As $r \to 1$ the modulation vanishes and the M_1^e mode is seen to turn smoothly into the M_1^c mode.) There exists a critical frequency $\omega_{c1}^e < \omega_{c1}^c$ at which the M_1^e mode gives rise to a modulated version of the M_2^c mode. The backward-forward cycles are here no more identical but their length becomes angle dependent. For increasing ω_H the average frequency $\bar{\omega}_r$ of the bound pair rotation does not follow the asymptotic ω_H^{-1} dependence found for the circularly polarized field. What we observe instead is that, as ω_H approaches a new critical value ω_{c2}^e, $\bar{\omega}_r$ goes to zero. Above ω_{c2}^e the pair is seen to exhibit but a simple oscillatory motion around a direction located between the long and short axes of the field ellipse. Let us denote this mode by M_3^e. As $\omega_H \to \infty$, the oscillatory motion vanishes and the average direction of the pair axis approaches the long axis of the ellipse. Both ω_{c1}^e and ω_{c2}^e are r dependent. As r decreases, the difference $(\omega_{c1}^e - \omega_{c2}^e)$ decreases. Below $r=0.5$ observations of the M_2^e mode, which exists in the range between those two critical frequencies, become practically impossible. The numerical solutions of Eq. (4) for two typical cases described above are shown in Figs. 2(e) and 2(f).

The experimental, analytical, and simulated results discussed so far are summarized in Fig. 3. In order to do this we have defined an *average* angular frequency of the rotating pair given as $\bar{\omega}_r = \omega_H - \omega_b/2$. In Fig. 3 we have also normalized the angular frequencies relative to ω_{c1}^c and the plot shows $\bar{\omega}_r/\omega_{c1}^c$ vs $\omega_H' = \omega_H/\omega_{c1}^c$ for different values of r. Experimental and simulated-analytical re-

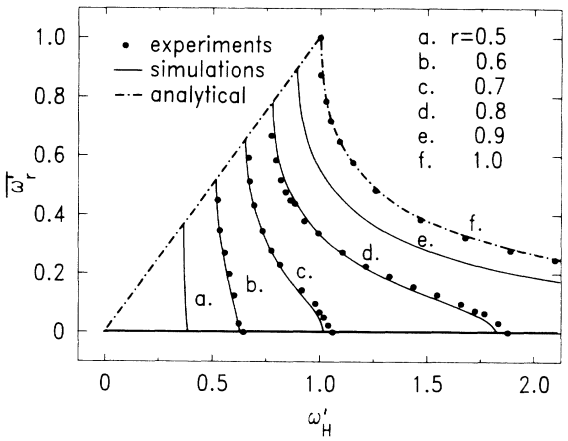

FIG. 3. Plots of the normalized average angular frequency $\bar{\omega}_r' = \bar{\omega}_r/\omega_{c1}^c$ for various amplitude ratios r of the components of the magnetic field vs the reduced angular frequency $\bar{\omega}_H' = \omega_H/\omega_{c1}^c$ for the rotating field. The solid curves represent simulated results and the dots experimental results. The dash-dotted curve for $r=1$ (curve f) is the exact analytical solution given by Eq. (6) and $\bar{\omega}_r' = (\omega_H - \omega_b/2)/\omega_{c1}^c$. The intersections of the solid curves a-e with the dash-dotted line to the left ($\bar{\omega}_r' = \omega_H'$) represent the critical frequencies ω_{c1}' in Fig. 4(a), whereas the intersections with the horizontal solid line ($\bar{\omega}_r' = 0$) represent the critical frequencies ω_{c2}' in Fig. 4(b).

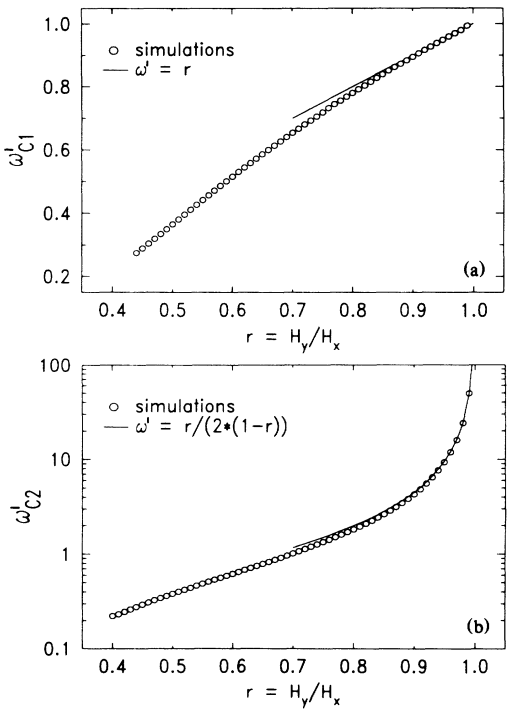

FIG. 4. (a) Behavior of the normalized lower critical angular frequency $\omega_{c1}' = \omega_{c1}^e/\omega_{c1}^c$ for different values of the anisotropy parameter r. The solid curve shows the asymptotic behavior for $r \to 1$. (b) Same as (a) for the normalized upper critical angular frequency $\omega_{c2}' = \omega_{c2}^e/\omega_{c1}^c$ with the solid curve indicating the asymptotic behavior as discussed in the text.

sults thus refer to here as measured and calculated values obtained for ω_b, respectively. As may be seen, the agreement is rather good except perhaps for ω_H' close to the ω_{c2}^e values. This is plausible as only very small deviations in the experimental setting of r from the nominal value will result in large deviations in the measured ω_b.

We have also investigated in detail the relationship between the anisotropy r and the lower and upper critical angular frequencies, ω_{c1}^e and ω_{c2}^e. These have been determined by an iterative approach. Figures 4(a) and 4(b) thus show the result of these computations (expressed relative to ω_{c1}^c). The curves showing the asymptotic behavior, for $r \rightarrow 1$, are based on rather lengthy evaluations of asymptotic behavior of integrals, and this is discussed elsewhere. As may be seen, ω_{c2}' ($=\omega_{c2}^e/\omega_{c1}^c$) diverges as $r \rightarrow 1$, so in the limit of circular driving fields, the pair will always rotate ($\bar{\omega}_r' > 0$) in our approximation, regardless of the values for ω_H'. By comparing Figs. 4(a) and 4(b) we also see that ω_{c1}' approaches ω_{c2}' as r decreases as also seen in Fig. 3.

From the present studies of rotating pairs of magnetic holes in a viscous fluid we are able to conclude that the dynamics are well described by an overdamped nonlinear equation of motion including magnetic and viscous torques. This is based on several cross checks between experimental results and numerical solutions. As the experimental system is rather simple and well defined, obvious extensions like the introduction of noise and frequency modulation of the driving field, allowing the particles to have radial motions, or the use of more than two particles should make it possible to study a wide range of nonlinear dynamic behavior including transition to chaos.

This research was supported in part by Dyno Industrier A/S and by the Norwegian Research Council for Science and the Humanities (NAVF). We would also like to thank J. Ugelstad, A. Berge, and T. Ellingsen for supplying the spheres used in the experiments and J. L. McCauley and J. P. Hansen for valuable discussions.

[1]R. W. Chantrell and E. P. Wohlfarth, J. Magn. Magn. Mater. **40**, 1 (1983).

[2]R. E. Rosensweig, Annu. Rev. Fluid Mech. **19**, 437 (1987).

[3]For cell separation and immunological analysis, see A. Berge, T. Ellingsen, K. Nustad, S. Funderud, and J. Ugelstad, in "Polymer Colloids," edited by R. H. Ottewill (Plenum, New York, to be published).

[4]A. R. Laufer, Am. J. Phys. **19**, 275 (1951).

[5]J. J. Newman and R. B. Yarbrough, J. Appl. Phys. **39**, 5566 (1968).

[6]D. Pfeffer and M. Gitterman, J. Magn. Magn. Mater. **68**, 243 (1987).

[7]A. T. Skjeltorp, Phys. Rev. Lett. **51**, 2306 (1983).

[8]A. T. Skjeltorp, J. Magn. Magn. Mater. **65**, 195 (1987).

[9]J. Ugelstad *et al.*, Adv. Colloid Interface Sci. **13**, 101 (1980). Produced by Dyno Particles A.S., N-2001 Lillestrøm, Norway.

[10]Type EMG 909 from Ferrofluidics Corp. with saturation magnetization $M_s = 200$ G, initial susceptibility $\chi = 0.0829$, and viscosity $\eta = 5$ cP.

[11]Surface charge effects were negligible for the present system. As it turned out, most spheres brought together by external fields and kept in contact for some time stayed together. The mechanism for this is not known.

[12]Equation (1) shows that whenever $\cos^2\theta < \frac{1}{3}$ the spheres repel each other which would lead to separation and more complicated trajectories.

[13]The Reynold's number is very low (typically $\mathrm{Re} \simeq 10^{-5}$) and experiments showed that Stokes' law applies with $K = 3\pi \times d_{\mathrm{eff}}$ and an effective diameter $d_{\mathrm{eff}} \simeq 1.75d$.

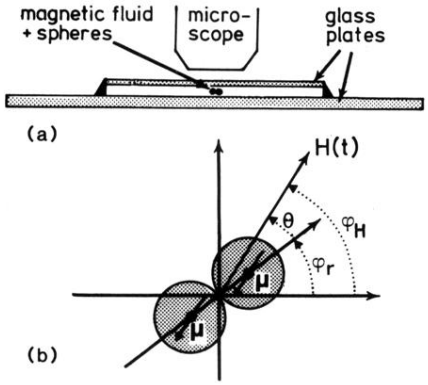

FIG. 1. (a) Sideview of the experimental setup. (b) Topview of the coordinate system for two magnetic holes rotating in the plane between the two glass plates in (a) and driven by the planar field $H(t)$ as discussed in the text.